Aggregation and Adsorption of Type I Collagen near an Electrified Interface

Stephanie D. Huelin,[†,‡] Holly R. Baker,[‡] Kristin M. Poduska,*[‡] and Erika F. Merschrod S.*[,†]

Department of Chemistry and Department of Physics and Physical Oceanography, Memorial University of Newfoundland, St. John's, NL A1B 3X7 Canada

Received June 26, 2007; Revised Manuscript Received August 29, 2007

ABSTRACT: An electric field can stimulate collagen fibrillogenesis in an acidic electrolyte, while unaggregated collagen monomers are preferentially adsorbed to the electrified interface itself. These effects are demonstrated using a Hull cell to apply an electric current gradient to 0.01 M HCl or 0.01 M HNO_3 containing collagen monomers. Atomic force microscopy and Raman scattering spectroscopy data show that collagen microfibrils form in the electrolyte and migrate toward the negatively charged working electrode. However, collagen monomers adsorb to the working electrode due in part to their faster electromigration rates. Despite the dramatic pH difference between the acidic bulk electrolyte (pH = 2) and the basic diffusion layer region in the immediate vicinity of the working electrode surface (pH > 10) due to base electrogeneration reactions in the aqueous electrolytes, there is no evidence that the electroadsorbed collagen monomers suffer from the effects of denaturation.

Introduction

Coatings that mimic the composition of natural biomaterials have a wide range of potential medical applications. For example, hydroxyapatite ($Ca_{10}(PO_4)_6(OH)_2$) is a compound that has been studied extensively because of its resemblance to the mineral phase in bone.[1,2] Adding collagen or other proteins to mineral coatings to form a bioinorganic composite material can increase the biocompatibility of the coating.[3,4] To this end, we describe how collagen, the most abundant protein in natural bone, aggregates near and adsorbs to an electrified interface. These results have potential applications to the formation of protein−mineral composite materials prepared by electrochemical, electrospinning, or electrospray methods.[5−9]

Collagen is a structural protein, and thus its function in the body corresponds to structural transformations through aggregation. Collagen aggregates, such as native type I collagen fibrils, are highly ordered. Ropelike collagen fibrils form from monomers in a complex, hierarchical process involving both axial and lateral aggregation of monomers and subsequent intermediate microfibrils.[10,11] The mechanism for the assembly of collagen monomers into fibrils is still a matter of active research, but it is widely believed that the neutralization of positive charge with increasing pH increases interactions among collagen monomers to form oligomers. Subsequent packing and fusing of oligomer intermediates lead to microfibrils (typically a few nanometers in diameter), which then assemble into larger fibrils (typically hundreds of nanometers to micrometers in diameter).[10] Early in the fibril formation process, intermediate aggregates are stabilized by polar, hydrophobic, and other noncovalent interactions. Aiding the study of this important biological assembly process is the fact that collagen fibrillogenesis can be induced in vitro with outcomes similar to those found in vivo.[11]

Collagen aggregation near electrified interfaces is a complex process which has not been widely studied. Collagen is a polyelectrolyte with localized regions of positive, negative, or effectively neutral charge due to the amino acid side chains.[12] These charges are pH dependent, with an overall positive charge (protonated amino acids) at acidic pH or an overall negative charge (deprotonated amino acids) at basic pH. Because collagen is charged, it can respond to the presence of an electric field through migration and alignment.[13] Migration in bulk electrolyte is dominated by electrophoretic flow, in which a species with net charge moves toward an oppositely charged electrode. This can result in adsorption of charged species at electrode surfaces, as has been observed for other types of proteins.[14,15] The situation can be further complicated by the presence of a pH gradient due to redox chemistry at the electrodes. In this case, the protein's net charge will change as it migrates until it becomes net neutral, at its isoelectric point.

Both migration and alignment can play a role in the electroaggregation of collagen, since the local orientation and concentration of monomers are understood to be essential in the formation of ordered fibrils. There are two well-established parameters for inducing in vitro aggregation of type I collagen: increased temperature (4−37 °C) to enhance reaction kinetics and ramped pH from acidic to neutral to enable charge associations between collagen monomers.[16] In the presence of an electric field, the charge association behavior can also be influenced by polyelectrolyte alignment.[17,18] For example, earlier studies have shown that collagen fibrils can be formed in high-voltage electrostatic fields.[19]

Our experiments investigate the effect of current density, electrolyte composition, and collagen concentration on the aggregation and migration of collagen near an electrified interface. In particular, we rank the effects of electric field and pH on electric-field-induced aggregation based on correlated spectroscopic, microscopic, and force curve data.

Experimental Methods

Electrolytes were made with bovine dermal type I collagen (Vitrogen stock solution, Cohesion Technologies/Inamed Biomaterials) in either 0.01 M HCl or 0.01 M HNO_3 (EMD, ACS Reagent grade) prepared with ultrapure water (Barnstead, 18.2 MΩ·cm).

* To whom correspondence should be addressed: e-mail erika@mun.ca, Fax 709-737-3702; e-mail kris@mun.ca, Fax 709-737-8739.
[†] Department of Chemistry.
[‡] Department of Physics and Physical Oceanography.

10.1021/ma0714159 CCC: $37.00
Published on Web 10/12/2007

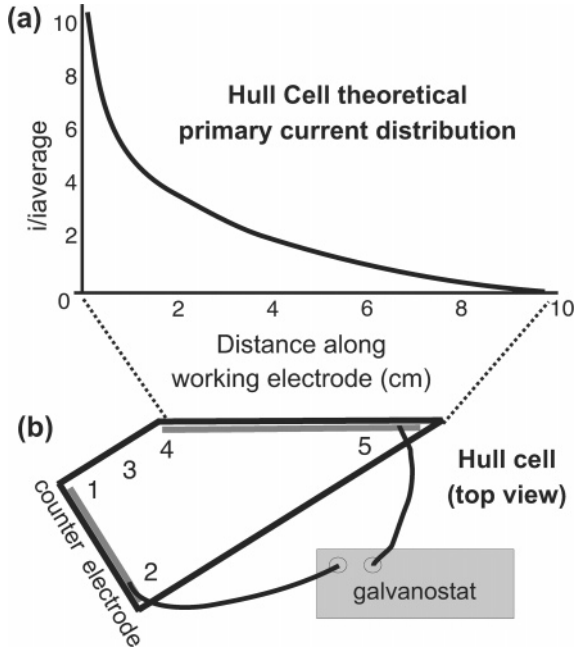

Figure 1. A logarithmic primary current distribution (a) along the working electrode led to a gradient in collagen adsorption. This was achieved in a modified Hull cell (b) in which the working electrode was angled at 51° with respect to the counter electrode. To assess collagen aggregation and migration within the electrolyte, aliquots were obtained ~5 mm away from the counter electrode at the high and low current density ends (points 1 and 2, respectively), midway between the two electrodes (point 3), and ~5 mm away the high and low current density ends of the working electrode (points 4 and 5, respectively).

The collagen concentrations used in this study (between 0.075 and 1.0 mg/mL) would lead to fibril formation under standard pH and temperature conditions for fibrillogenesis in vitro.[11] Our choice of supporting electrolytes was influenced by the fact that HNO_3 is the dominant component of an electrolyte that has recently been used for electrochemically assisted calcium phosphate coatings,[8] while HCl provides a redox-inactive reference point under the conditions of our experiments.

For the collagen aggregation and adsorption experiments, a standard 250 mL Hull cell,[20,21] shown schematically in Figure 1, allowed sampling of a range of current densities in a single experiment with its angled counter and working electrodes. The distance between working and counter electrodes ranged from 4.8 cm at the closest point to 12.7 cm at the furthest. The logarithmic trend in the scaled current density as a function of distance, shown in Figure 1a, is a general feature of Hull cells; the actual unscaled current densities would vary with electrolyte composition and cell dimensions.[20,21] Our experiments encompassed a range of average cathodic current densities (−0.5 to −1.5 mA/cm^2), applied for 30 min. These current densities correspond to applied potentials in the range of −2 to −4 V vs a saturated calomel (SCE) reference. A smaller (3.5 mL) glass electrochemical cell, with parallel electrodes 2.5 cm apart, was constructed for in situ optical detection of collagen aggregation under crossed polarizers and to facilitate microscopic spatial measurements of pH gradients near the working electrode surface. Manually polished, corrosion-resistant stainless steel was used for all electrodes.

Collagen aggregation and migration were assessed using data from complementary morphological, spectroscopic, and optical techniques. Collagen monomers are flexible structures approximately 300 nm long and 1.5 nm in diameter, while collagen fibrils are typically 1−10 μm long and 20−200 nm wide. Thus, aggregation and fibrillogenesis information can be obtained from collagen feature sizes using atomic force microscopy (AFM) imaging.[22] All AFM imaging was carried out with an Asylum Research MFP-3D system using silicon cantilevers with aluminum-coated backsides (force constant ~7.5 N/m, Mikromasch). A scan speed of 0.5−5.0 μm/s provided low noise with a reasonable data collection time. Images are shown with no postprocessing beyond a simple plane fit and present morphology deemed typical on the basis of numerous replicate experiments. Force curve data, to assess collagen aggregate types according to elasticity and adhesion, were obtained with the same instrument, but with an uncoated silicon cantilever (force constant 0.84 N/m, Mikromasch).

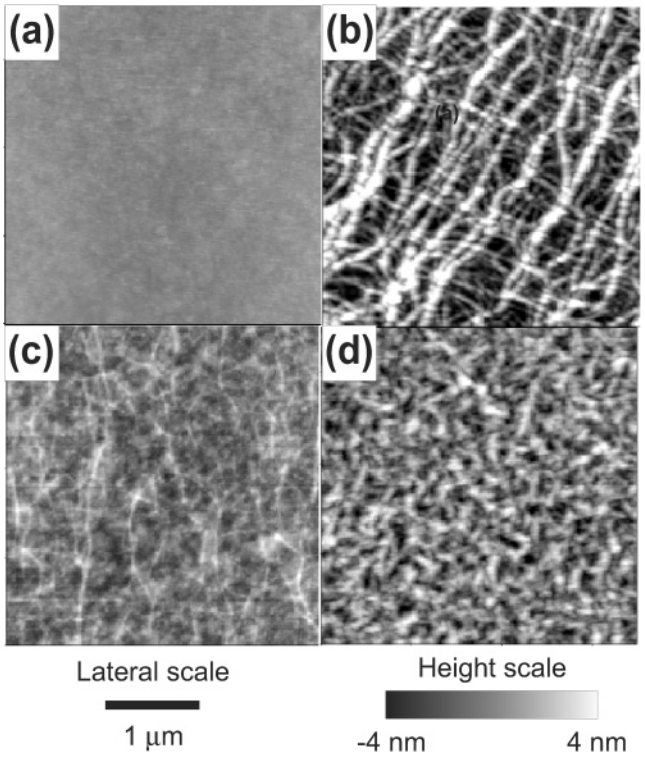

Figure 2. Comparison of representative AFM images of air-dried collagen taken from different points in the Hull cell after 30 min of current flow (electrolyte: 0.15 mg/mL collagen in 0.01 M HNO_3). Image (a) shows no collagen near the counter electrode, while large collagen fibrils were present midway between the electrodes (b). Closer to the working electrode, the morphology of the aggregated collagen was qualitatively different near the low (c) and high (d) current density ends.

Supporting data, based on changes in the vibrational properties of the collagen, were obtained from Raman scattering spectroscopy (confocal configuration with 532 nm excitation, LabRAM, Jobin Yvon Horiba). Spectroscopic analyses were applied to both collagen sampled from the electrolyte (dried on mica using filtered compressed air) and collagen adsorbed to the working electrode surface (air-dried). Finally, in situ optical detection of collagen aggregation and alignment was facilitated with polarized light microscopy (Leica DM2500 with polarized light capability).

Results and Discussion

Aggregation and Migration of Electrolyte-Based Collagen. Electrolyte aliquots were removed from five positions within the Hull cell, as indicated by the numbers in Figure 1b, then placed on mica surfaces, air-dried, and imaged with AFM. Representative images are shown in Figure 2, and results were similar in both HNO_3 and HCl electrolytes. After 30 min of current flow, there was no evidence of protein monomers, much less fibril formation, next to the counter electrode (Figure 2a). However, there were many fibrils present midway between the electrodes (Figure 2b). In the high current density end of the cell, this midway region contained the thickest fibrils, and there was evidence of banding (indicative of a more hierarchical structure[23]) on fibrils prepared in some experiments. Collagen was also present in the electrolyte near the working electrode.

Fibrils near the low current density end of the working electrode (Figure 2c) tended to be smaller than those observed in mid-cell (Figure 2b). The collagen present near the high current density end (Figure 2d) shows a qualitatively different morphology, consisting of more globular aggregates. These trends in fibril formation and migration were similar over the entire range of collagen concentrations (0.075−1.0 mg/mL), indicating that the magnitude of the current density plays a more dominant role than initial collagen concentration in determining the distribution and form of collagen throughout the electrolyte.

Despite the fact that our experiments are conducted in an electrolyte whose bulk pH remains acidic (pH = 2), we nevertheless observe collagen aggregation in these acidic regions. Collagen-containing electrolytes which remained in the Hull cell for an equivalent amount of time but without an applied field showed no evidence of fibril formation (as would be expected at pH 2), indicating that the applied field is inducing fibrillogenesis. Analogous to the effects of a pH ramp, the applied field changes the propensity for collagen aggregation through charge associations between ions in the electrolyte and the collagen which screen the net positive charge of the protein.

To explain the size differences, despite being at the same pH, between the larger fibrils observed midway between the electrodes and the smaller fibrils detected near the working electrode surface, the relative mobilities of different forms of collagen must be taken into account. Under the acidic pH conditions used in our experiments, collagen has an overall positive charge and thus moves toward the negative (working) electrode. (We note that electroosmotic mobility of the solvent, resulting from ion interactions with vessel walls, does not have a significant impact on collagen migration in our experiments because the double layer resulting from this interaction is very small compared to the size of our electrochemical cell.) Given that there will be localized regions of negative and neutral charge on the collagen, its migration behavior could be complex. However, our results clearly show a net collagen migration toward the negatively charged working electrode; no collagen was detected next to the counter electrode, while a dense network was seen next to the working electrode. Larger aggregates also have a higher degree charge compensation through electrostatic associations of the component monomers, which further reduce their electromobility.

Earlier work has shown that collagen is mainly oriented in an electric field by its large permanent dipole, caused by its uneven charge distribution, and to a much lesser extent by anisotropy of proton fluctuations and polarization of the ion atmosphere.[13] Alignment of these dipoles can facilitate electrostatically driven assembly of oligomers and fibrils.[24] Using in situ polarized light microscopy, visual signatures of collagen alignment were not evident, even after 30 min of electromigration. However, supporting experiments under pH and potential conditions for which the protein was very localized spatially, and thus was present in much higher density, did show light rotation due to collagen alignment.

Electroadsorption of Collagen. The current density gradient enabled by the Hull cell resulted in an electroadsorbed collagen film with a thickness gradient along the length of the working electrode, with the thickest films at the high current density end. Significant electrically induced collagen adsorption required current densities greater than 5 mA/cm^2. The largest current densities used in our studies (15 mA/cm^2) yield collagen films 450−650 nm thick after 30 min of current flow. Figure 3 shows a representative AFM image of an electroadsorbed collagen film prepared at 6 mA/cm^2 that emphasizes both the absence of

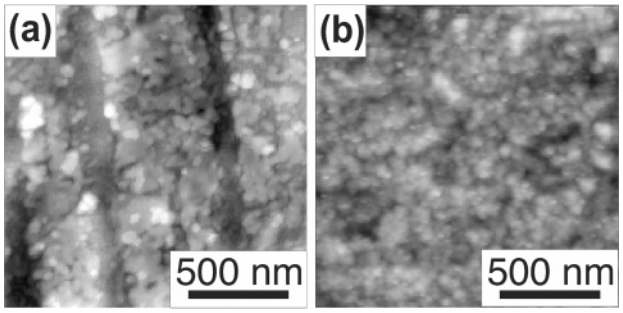

Figure 3. Representative AFM images of (a) bare mechanically polished stainless steel and (b) electroadsorbed collagen on stainless steel after 30 min of applied current to an electrolyte containing 0.075 mg/mL collagen in 0.01 M HCl.

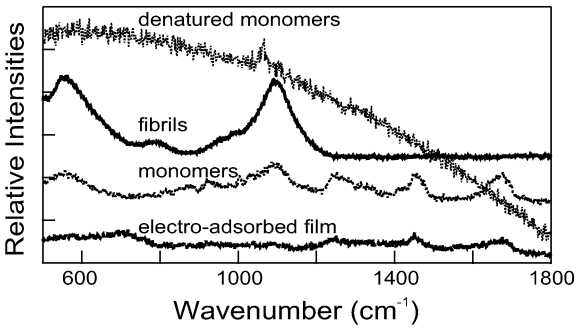

Figure 4. Representative Raman scattering spectra from collagen monomers, collagen fibrils, denatured collagen, and the electroadsorbed collagen film. The spectroscopic signatures of the electroadsorbed collagen most closely resemble those for collagen monomers, especially in the 1000−1800 wavenumber region.[25]

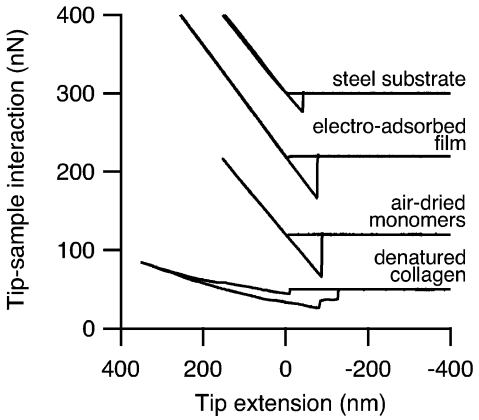

Figure 5. Force curve comparisons show that electroadsorbed collagen has the same mechanical properties as intact collagen monomers. In stark contrast, denatured collagen has a very complex, multistage pull-off behavior with large hysteresis.

fibrillar collagen and the uniformity of film coverage relative to the underlying undulations of the stainless steel substrate. The electroadsorbed collagen has a more globular morphology relative to the fibrils observed in the nearby electrolyte (Figure 2c). While this globular morphology could suggest collagen denaturation, Raman spectroscopic data (Figure 4) indicate that the electroadsorbed collagen is most similar to monomers, with little similarity to the spectroscopic signatures of denatured collagen. Force curves of base-denatured collagen, air-dried collagen monomers, and electroadsorbed collagen show that the electroadsorbed collagen film does not have the complex, multistage pull-off behavior seen for denatured collagen (Figure 5). These trends in the morphological and spectroscopic data for electroadsorbed collagen films were similar over the entire

range of collagen concentrations (0.075−1.0 mg/mL) in both the HNO_3 and HCl electrolytes.

Our data suggest that the morphological differences between the electroadsorbed collagen and the fibrils in the electrolyte have a two-part origin. First, migration rate differences between monomers and fibrils lead to higher monomer concentrations in the immediate vicinity of the working electrode surface. Second, pH changes at the electrified interface instigate rapid, globular aggregation of these monomers, where the very basic pH would not facilitate fibrillogenesis.

In our electrochemical cell, a diffusion layer—depleted of oxidized species—exists very close to the working electrode as a result of the electrochemistry of water and/or nitrate ions.[26] (The oxidation of chloride ions is not favorable under our experimental conditions.) Water electrolysis generates more basic conditions near the working electrode and more acidic conditions near the counter electrode:

working electrode (cathode):

$$2H_2O(l) + 2e^- \rightarrow H_2(g) + 2OH^-(aq) \qquad (E^\circ = -1.072 \text{ V vs SCE})$$

counter electrode (anode):

$$2H_2O(l) \rightarrow O_2(g) + 4H^+(aq) + 4e^- \qquad (E^\circ = +1.472 \text{ V vs SCE})$$

In addition, nitrate (when present) is easily reduced at the working electrode surface:

$$NO_3^-(aq) + H_2O(l) + 2e^- \rightarrow NO_2^-(aq) + 2OH^-(aq) \qquad (E^\circ = -0.142 \text{ V vs SCE})$$

Both the water and nitrate reactions lead to more basic pH conditions in the immediate vicinity of the working electrode surface. In situ optical microscopy studies of the cell containing a universal pH indicator, complemented by independent micro pH electrode measurements, suggest that this basic pH region is confined to within 50 μm of the working electrode surface and that its pH value is greater than 10. This is reasonable given the mobilities of the hydroxide ions[27] and the rate of formation based on current measured at the working electrode. It is important to note that, while oxidation and reduction reactions are important for localized pH changes in our electrolyte, collagen itself is not redox active.[28]

The morphological and Raman spectroscopic data (Figures 3 and 4) suggest preferential electroadsorption of monomers to the working electrode surface. Collagen fibrils have an experimental diffusion coefficient of about 0.45×10^{-7} cm^2/s (based on a weighted average of 2.85 monomers per aggregate) while individual monomers have a theoretical diffusion coefficient that is nearly twice as large (0.858×10^{-7} cm^2/s).[29] Thus, it is reasonable to expect that monomers will be present near the working electrode at a higher density compared to the larger, slower-moving fibrils.

Once collagen monomers enter the diffusion layer region, basic pH conditions could cause denaturation. Alternatively, since fibrillogenesis results from increasing pH from acidic to neutral, it is conceivable that the pH increase near the working electrode could favor collagen aggregation.[16] Our results show that a third option is possible. We see that a sharp pH interface does not promote the fibrillogenesis observed from a slower pH ramp,[30] consistent with other studies in our group that have shown that a rapid pH increase, comparable to the conditions experienced by electromigrating collagen monomers, does not promote fibrillogenesis. However, the globular aggregates we observe are substantially larger than collagen monomers, thus indicating a different aggregration or charge association process.

It is worth emphasizing the practical significance of collagen monomer electroadsorption without denaturation. While the fibrillar form of collagen has been found to be less susceptible to base-induced denaturation (gelation) than monomers,[30] it is remarkable that monomers are able to withstand the high-pH regions found near the working electrode. It is plausible that this could be due in part to prior nonspecific associations within the electrolyte. With this capability to form monomer films, one can therefore tune the texture and hence bioactivity of the resulting coating.

Conclusions

Our results show that an electric field can stimulate collagen fibrillogenesis in an acidic electrolyte but that monomers (the unaggregated form of collagen) are preferentially adsorbed to the electrified interface itself. Given the higher mobility of collagen monomers relative to the larger collagen fibrils or aggregates, it is reasonable to expect a higher concentration of collagen monomers near the working electrode surface. Despite the dramatic pH differences between the acidic bulk electrolyte (pH = 2) and the basic diffusion layer region in immediate vicinity of the working electrode surface (pH > 10), there is no evidence that the electroadsorbed collagen monomers suffer from the effects of denaturation. This suggests that electric fields may be an effective method for creating collagen coatings as well as collagen−mineral composite coatings.

Acknowledgment. The authors thank Y. H. Lee (Biology) and Dr. K. Nag (Biochemistry) for the use of materials characterization facilities at Memorial University of Newfoundland. This work was supported by the Natural Sciences and Engineering Research Council of Canada (Discovery Grants for K.M.P. and E.F.M.S. and Undergraduate Student Research Awards for S.D.H.), the Canada Foundation for Innovation, the Industrial Research and Innovation Fund, and Memorial University of Newfoundland.

References and Notes

(1) Ben-Nissan, B. *MRS Bull.* **2004**, *29*, 28−32.
(2) Vallet-Regí, M.; González-Calbet, J. M. *Prog. Solid State Chem.* **2004**, *32*, 1−31.
(3) Wang, J.; de Boer, J.; de Groot, K. *J. Dent. Res.* **2004**, *83*, 296−301.
(4) Kikuchi, M.; Itoh, S.; Ichinose, S.; Shinomiya, K.; Tanaka, J. *Biomaterials* **2001**, *22*, 1705−1711.
(5) Zhitomirsky, I. *Adv. Colloid Interface Sci.* **2002**, *97*, 279−317.
(6) Cheng, X.; Filiaggi, M.; Roscoe, S. G. *Biomaterials* **2004**, *25*, 5395−5403.
(7) Fan, Y.; Duan, K.; Wang, R. *Biomaterials* **2005**, *26*, 1623−1632.
(8) Huelin, S. D.; Baker, H. R.; Merschrod, S. E. F.; Poduska, K. M. *Cryst. Growth Des.* **2006**, *6*, 2634−2636.
(9) Thomas, V.; Dean, D. R.; Jose, M. V.; Matthew, B.; Chowdhury, S.; Vohra, Y. K. *Biomacromolecules* **2007**, *8*, 631−637.
(10) Goh, M. C.; Paige, M. F.; Gale, M. A.; Yadegari, I.; Edirisinghe, M.; Strezelczyk, J. *Physica A* **1997**, *239*, 95−102.
(11) Kadler, K. E.; Holmes, D. F.; Trotter, J. A.; Chapman, J. A. *Biochem. J.* **1996**, *316*, 1−11.
(12) Rainey, J. K.; Goh, M. C. *Protein Sci.* **2002**, *11*, 2748−2754.
(13) Porschke, D. *Annu. Rev. Phys. Chem.* **1985**, *36*, 159−178.
(14) Cosman, N. P.; Roscoe, S. G. *Langmuir* **2004**, *20*, 1711−1720.
(15) Burgess, I.; Li, M.; Horswell, S. L.; Szymanski, G.; Lipkowski, J.; Satija, S.; Majewski, J. *Colloids Surf., B* **2005**, *40*, 117−122.
(16) Nimni, M. E. *Collagen*; CRC Press: Boca Raton, FL, 1988.
(17) Worley, C. G.; Linton, R. W.; Samulski, E. T. *Langmuir* **1995**, *11*, 3805−3810.
(18) Chao, C.-Y.; Li, X.; Ober, C. K.; Osuji, C.; Thomas, E. L. *Adv. Funct. Mater.* **2004**, *83*, 364−370.

(19) Kidoaki, S.; Kwon, I. K.; Matsuda, T. *Biomaterials* **2006**, *25*, 37−46.
(20) Hull, R. O. *Mon. Rev. Am. Electroplaters' Soc.* **1939**, 753−767.
(21) Nohse, W. *The Investigation of Electroplating and Related Solutions with the Aid of the Hull Cell*; Robert Draper Ltd.: Teddington, England, 1966.
(22) Dufrene, Y. F.; Marchal, T. G.; Rouxhet, P. G. *Langmuir* **1999**, *15*, 2871−2878.
(23) Ottani, V.; Martini, D.; Franchi, M.; Ruggeri, A.; Raspanti, M. *Micron* **2002**, *33*, 587−596.
(24) Köster, S.; Leach, J. B.; Struth, B.; Pfohl, T.; Wong, J. Y. *Langmuir* **2007**, *23*, 357−359.
(25) Xu, J.; Stangel, I.; Butler, I.; Gilson, D. *J. Dent. Res.* **1997**, *76*, 596−601.
(26) Parr, J. G.; Beddoes, J. *Introduction to Stainless Steels*, 3rd ed.; ASM International: Materials Park, OH, 1999.
(27) Weast, R. C. *Handbook of Chemistry and Physics*, 50th ed.; CRC Press: Boca Raton, FL, 1969.
(28) Dey, S. K.; Long, Y.-T.; Chowdhury, S.; Sutherland, T. C.; Mandal, H. S.; Krantz, H.-B. *Langmuir* **2007**, *23*, 6475−6477.
(29) Silver, F. H.; Trelstad, R. L. *J. Biol. Chem.* **1980**, *255*, 9427−9433.
(30) Wood, G. C. *Biochem. J.* **1960**, *75*, 598−605.

MA0714159